

Flux-pinning properties of single crystalline and dense polycrystalline MgB₂

Z. X. Shi, A. K. Pradhan, M. Tokunaga, K. Yamazaki, and T. Tamegai*

Department of Applied Physics, The University of Tokyo, 7-3-1 Hongo, Bunkyo-ku, Tokyo 113-8656, Japan

Y. Takano and K. Togano

*National Institute for Materials Science, 1-2-1 Sengen, Tsukuba 305-0047, Japan**and CREST, Japan Science and Technology Corporation, 2-1-6 Sengen, Tsukuba 305-0047, Japan*

H. Kito and H. Ihara

National Institute of Advanced Industrial Science and Technology, 1-1-1 Umezono, Tsukuba 305-8568, Japan

(Received 19 September 2002; revised manuscript received 12 June 2003; published 18 September 2003)

Magnetic hysteresis loops (MHLs) have been measured on single-crystalline and dense polycrystalline MgB₂ prepared under high pressure by micro-Hall probe and superconducting quantum interference device magnetometer. Heating effect due to the viscous force on vortices has been found by changing the field-sweep rate. Magnetic critical current densities obtained from MHLs by Bean model show different field dependence for single and polycrystalline samples. The scaling behaviors of flux-pinning force are also different. There is only one pinning force peak for polycrystalline sample, whereas there are three pinning force peaks for single-crystalline sample. The irreversibility field has been determined by different methods. The anisotropy of flux pinning and the pinning mechanism in MgB₂ are discussed.

DOI: 10.1103/PhysRevB.68.104514

PACS number(s): 74.25.Qt, 74.25.Sv, 74.25.Op

I. INTRODUCTION

Since the discovery of superconductivity in MgB₂,¹ many experiments on polycrystalline bulks and thin films have established some of its fundamental properties and demonstrated the possibility for application with strongly linked intergrains.^{2,3} However, the flux-pinning mechanism which governs the critical current density and the irreversibility field is still under investigation, and is very important to the practical application of MgB₂. The field and temperature dependence of critical current density and flux-pinning force is the key to the understanding of flux-pinning mechanism in MgB₂. Some groups have reported their data on polycrystalline samples. For example, Larbalestier *et al.* reported a Kramer scaling behavior of flux-pinning force,² Kim *et al.* reported an exponential field dependence of critical current density,⁴ and Dou *et al.* reported exponential and power field dependent J_c .^{5,6} Almost all data reported by now show linear temperature dependence of critical current density. However, all these experiments were done on polycrystalline sample and these relations may be the mixture of the out-of-plane and in-plane contributions. So these relations may not be suitable and accurate enough for discussing the pinning mechanism due to the influence of the anisotropy of MgB₂ with layered structure. High-quality single-crystalline samples are indispensable to access intrinsic properties of MgB₂. The field and temperature dependence of critical current densities and flux-pinning force should also be measured on single-crystalline samples to avoid the grain-orientation problem. Since the single-crystalline sample was prepared, some structural examination and transition measurements have been performed.⁷⁻¹⁰ However, only a few papers have been reported on the pinning mechanism in single-crystal MgB₂.¹¹⁻¹³ Furthermore, the anisotropic properties of flux-pinning are also very important for the clarification of the

flux-pinning mechanism and the application of MgB₂. In this paper, we report our systematic and comparative studies of flux-pinning properties in single-crystalline and dense polycrystalline MgB₂ samples, such as critical current density, flux-pinning force, the irreversibility field, and the anisotropy.

II. EXPERIMENT

Our polycrystalline sample was synthesized under high pressure at high temperature as described in Ref. 14. The x-ray-diffraction analyses show that there is only single phase in our samples with almost theoretical density of 2.63 g/cm³. T_c is about 38 K and the transition width is less than 1 K. The high-resolution polarizing microscope observations reveal grains of size 50–200 μm. The polycrystalline sample is a polished rectangular sample. The single-crystalline sample is a platelet extracted near the surface of a large bulk sample, which we extracted polycrystalline sample also from the center. The sizes of two samples investigated here are 430×230×85 μm³ and 340×230×95 μm³, respectively. Magnetic hysteresis loops (MHLs) at different temperatures have been measured by both micro-Hall probe and superconducting quantum interference device (SQUID) magnetometer. The sensing area of Hall probe is 20×20 μm² and the field resolution is better than 0.01 G. The angular dependence of the upper critical field H_{c2} and irreversibility has been deduced from superconducting transition curves measured by standard four-probe transport measurement with magnetic field applied at different angles from c axis. Details of experiments are described in Ref. 15.

III. RESULTS AND DISCUSSION**A. Heating effect**

As reported in many papers,^{5,16,17} flux jumps in MHLs demonstrate the thermomagnetic instability in MgB₂, which

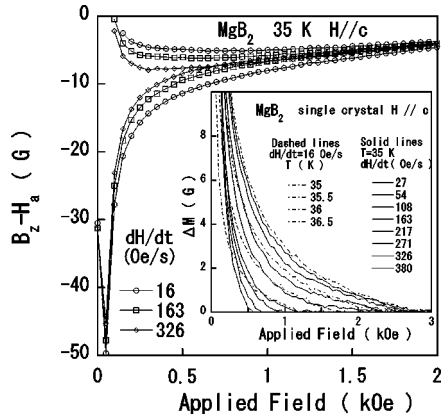


FIG. 1. MHLs measured by Hall probe with different field-sweep rates on single-crystal sample. Inset shows the field-dependent hysteresis width ΔM from MHLs measured at 35 K for different field-sweep rates (solid lines) and from MHLs measured at different temperatures near 35 K with $dH/dt=16$ Oe/s (dashed lines).

may be resulted from high viscous force and low thermal conductivity. The heat released by moving vortices causes local temperature rise. By changing the field-sweep rate, we have successfully found the heating effect on MHL as shown in Fig. 1. The local field hysteresis were measured by changing the field step by step at constant field-sweep rates. At every step the local field was measured in very short time after the field was stabilized. The MHL with slower field-sweep rate is fatter than that with faster-field sweep rate, which is contrary to the case caused by magnetic relaxation. Systematic measurements have been performed on single-crystal sample at 35 K, 20 K, and 5 K using Hall probe. Figure 1 shows the typical data at 35 K. The field dependence of the width of magnetic hysteresis ΔM as well as the irreversibility field are different for MHLs with different field-sweep rate. Though ΔM decreases with increasing temperature or field-sweep rate, the field dependence of ΔM is different for these two cases, as shown in the inset of Fig. 1. At lower fields, ΔM at 35 K with higher field-sweep rate is larger than ΔM at higher temperatures with lower field-sweep rate. However, at higher fields, the ΔM at 35 K with higher field-sweep rate is close to the ΔM at some higher temperature with slower field-sweep rate. The reason may be that flux-pinning force changes with field and results in heating effect changing with field also. So it is very important to measure the MHL at fixed temperature without heating effect so as to deduce the real field dependence of ΔM .

Figure 2 shows the change of ΔM at different field-sweep rate at 35 K, 20 K, 5 K for different field steps ΔH . With small field step, such as $\Delta H=10$ Oe, the change of ΔM saturates because heating time is short at each step and the total heat is small compared to the heat capacity. So the largest change of temperature of the sample, ΔT , is limited and the change of ΔM saturates at higher field-sweep rate. With larger field step, such as $\Delta H=200$ Oe, the time for each step is long enough for the sample to reach the steady state, and the sweep-rate dependent temperature distribution can be attained. So the change of temperature ΔT depends

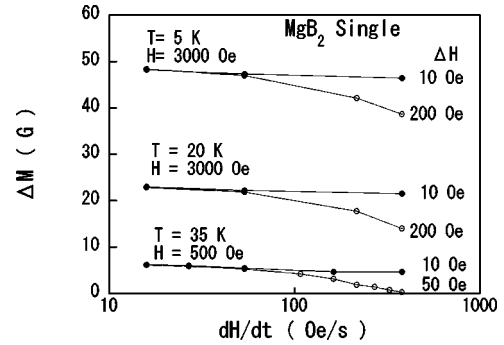


FIG. 2. Width of magnetic hysteresis ΔM at constant field. It changes with field-sweep rates (by different steps) at different temperatures.

on the field-sweep rate. Of course, it will saturate at some very high field-sweep rate also. The relative change of ΔM is larger at higher temperatures. So both heating effect and flux relaxation are serious at higher temperatures and strongly affect the measurement of MHLs.

B. Critical current density and flux pinning

By measuring the MHLs with slow field-sweep rate, we have performed the quasistatic measurements and have obtained quasi-critical-state MHLs as shown in Fig. 3. The polycrystalline sample was measured by SQUID magnetometer and the single-crystalline sample was measured by both Hall probe and SQUID magnetometer. The shape of MHLs of single crystal is different from that of polycrystalline samples and similar to that of powder samples.¹⁴ The

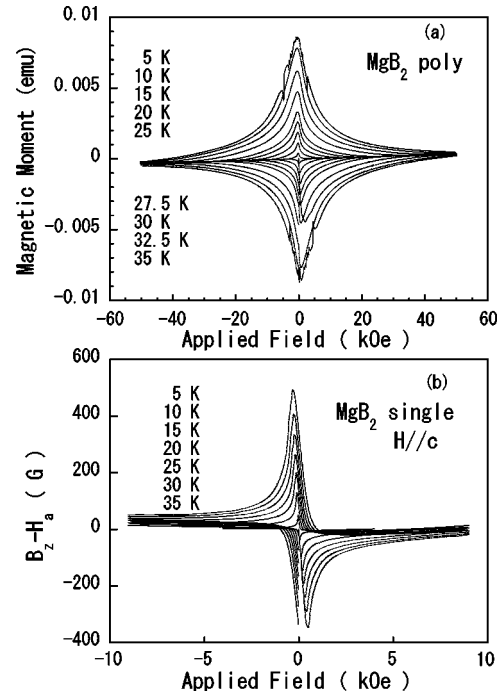


FIG. 3. MHLs measured at different temperatures on (a) polycrystalline sample by SQUID magnetometer and (b) single-crystal sample by Hall probe.

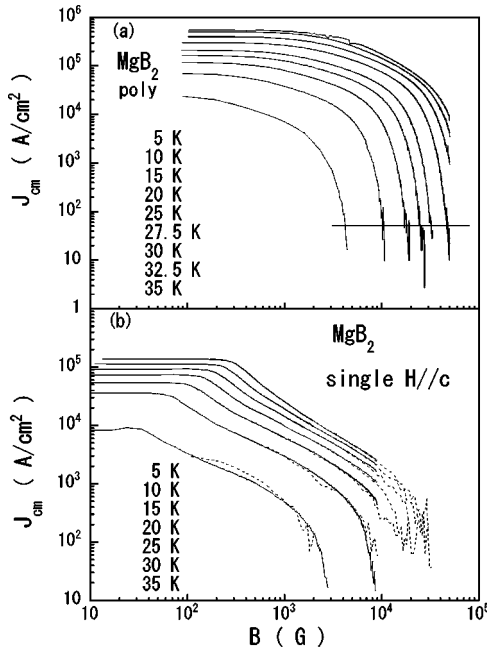


FIG. 4. Field-dependent critical current density J_{cm} at different temperatures calculated by Bean model from MHLs measured on (a) polycrystalline sample by SQUID magnetometer and (b) single-crystal sample by Hall probe (solid lines) and SQUID magnetometer (dashed lines).

peak of MHL for single crystal is much sharper than the peak for polycrystalline sample, which may be related to the surface pinning as well as the surface superconductivity in MgB_2 ,¹⁵ and the details will be discussed later.

Using Bean model, the magnetic critical current density J_{cm} can be deduced from MHLs at different temperatures. Figures 4(a) and 4(b) show the field dependence of magnetic critical current density J_{cm} for polycrystalline and single-crystalline samples, respectively. Though J_{cm} is almost field independent at lower fields for single-crystalline and polycrystalline samples, the field dependence of J_{cm} at higher fields is quite different for the two kinds of samples. In polycrystalline sample, J_{cm} sustains large values at intermediate fields and is suppressed rapidly at higher fields, which is due to the fact that grains with c axis parallel to the applied field change into normal state. In single-crystal sample, J_{cm} has power-law field dependence at intermediate fields and exponential field dependence at higher fields, which is shown in the inset of Fig. 5(b) clearly by fitting the scaling behavior of J_{cm} . This field dependence is also quite different from the data reported by other groups²⁻⁶ on polycrystalline samples. J_{cm} close to zero field shows almost linear temperature dependence for both single-crystalline and polycrystalline samples, as shown in Figs. 5(a) and 5(b), and is consistent with the results reported in Ref. 18.

From Figs. 4(a) and 4(b) the flux-pinning force, $F_p = (1/c)J_c \cdot B$, can be calculated and the scaling behavior of pinning force is shown in Figs. 6(a) and 6(b). The scaling behavior is also quite different for the two kinds of samples. For polycrystalline sample, the scaling is not good especially at higher fields due to the dispersion of grain orientations and

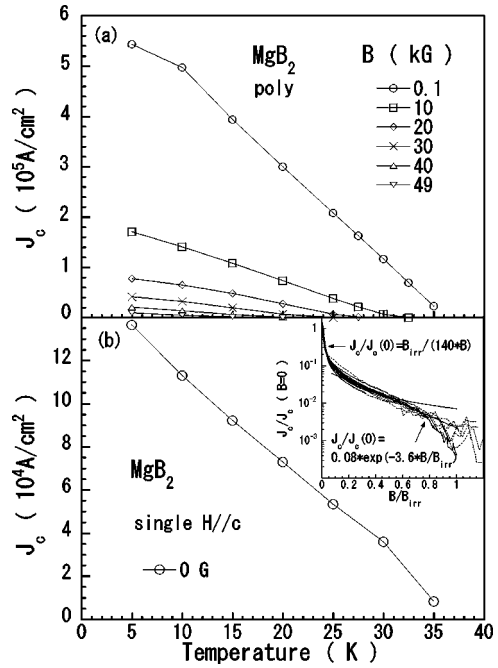


FIG. 5. Temperature dependence of J_{cm} at constant field for (a) polycrystalline and (b) single-crystalline samples. The inset of (b) shows the scaling behavior of J_{cm} . In intermediate fields J_{cm} has power field-dependence while in higher fields J_{cm} has exponential field dependence.

the anisotropy of the upper critical field. This is quite different from the reports by Kim *et al.*⁴ and Larbalestier *et al.*,² where they claim a good scaling of flux-pinning force for polycrystalline samples. At higher temperatures near T_c , the value of $\gamma = H_{c2}^{ab}/H_{c2}^c$ is small and the difference between H_{c2}^{ab} and H_{c2}^c is also small. However at lower temperatures, the value of γ is larger and H_{c2}^{ab} is much higher than H_{c2}^c . So it seems unreasonable to expect a good scaling of flux-pinning force for polycrystalline samples.

As shown in Fig. 6(b), the scaling behavior of flux-pinning force is better for single-crystalline sample. There is only one pinning force peak for polycrystalline sample, whereas there are three pinning force peaks for single-crystalline sample. The shape of scaled main peaks are similar for both samples, and they can be fitted by Kramer model,¹⁹ $f_p(h) \propto h^{1/2}(1-h)^2$, approximately except for the deviation at lower and higher fields due to the peaks near zero field and H_{c2}^c . The scaling behavior of the near zero-field peak is shown in the inset of Fig. 6(b). The temperature dependences of the peak position and the peak value are shown in Fig. 7. Though the pinning force density of polycrystalline sample is about two orders of magnitude higher than that of single-crystalline sample, the temperature dependence is almost the same for main peaks, while the near zero-field peak has different temperature dependence possibly due to the different pinning mechanism. The temperature dependence of the peak positions is almost linear except for the abnormal downturn at lower temperatures for polycrystalline sample, as shown in the inset of Fig. 7. This strange behavior can be explained as follows: Though the near zero-field peak and the main peak are separated clearly for single-

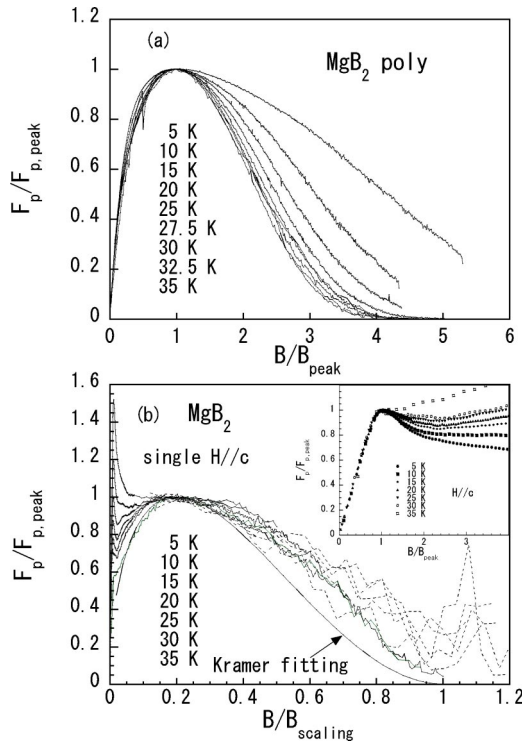


FIG. 6. Scaling behavior of flux-pinning force in (a) polycrystalline sample and (b) single-crystal. Inset of (b) shows the scaling behavior of flux-pinning force peaks near zero field.

crystalline sample, these two peaks are mixed together due to the dispersion of grain orientations for polycrystalline sample. These two peaks affect each other and result in the broadened peaks together with the distribution of upper critical fields. The peak position is shifted to lower fields especially at lower temperatures. Another possible reason is the influence of flux jump at lower temperatures on the critical-current densities.

As to the high-field peak near H_{c2}^c , we have reported it in Ref. 20, which was followed by the report of the peak effect in transport measurement near H_{c2} by Welp *et al.*,²¹ peaks in MHLs by Angst *et al.*,²² and similar peaks by Lyard *et al.*²³ We have confirmed the peak effect again by measuring MHL with field applied at 0° and 45° from c axis by SQUID magnetometer. A clear peak effect is observed only at lower temperatures with $H//c$ axis, as shown in Fig. 8. No peaks

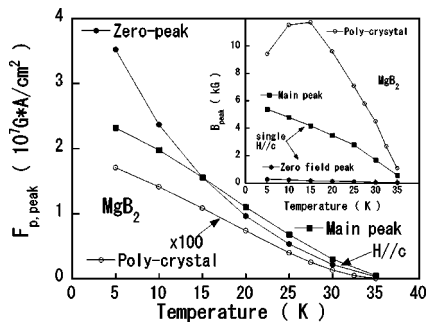


FIG. 7. Temperature dependence of the value and position (inset) of flux-pinning force peaks in Fig. 6.

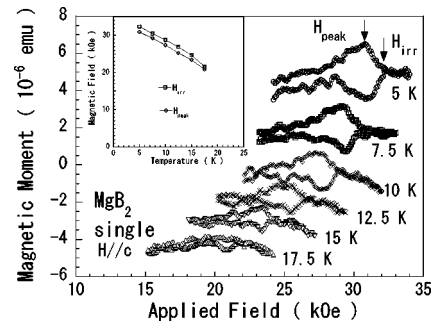


FIG. 8. High-field peaks near H_{c2} in MHLs measured at different temperatures with magnetic field parallel to c axis by SQUID magnetometer. Inset shows the temperature dependence of peak fields and irreversibility fields.

are found with field applied at 45° from c axis, in contrast to the result in Ref. 22. The temperature dependence of the peak position and the irreversibility field defined by closing points of MHLs are shown in the inset of Fig. 8. The peak effect may be caused by the softening of vortex lattice near H_{c2} , where vortices can adjust their positions to pinning centers to earn pinning energy. Alternatively, the vortex state may have changed by the so-called disorder-induced phase transition from disorder-free Bragg glass to disordered glass state.²⁴

From the above data, the irreversibility field H_{irr} can be deduced and summarized in Fig. 9. The H_{irr} is determined by a criterion of $J_c = 40 \text{ A/cm}^2$ as shown in Fig. 4(a), the closing points of MHLs as shown in Fig. 8, the scaling behavior of pinning force as shown in Fig. 6(b), as well as the end points of phase-transition curves (zero points of $\partial M/\partial T$) as reported in our previous paper.¹⁵ The data of H_{c3}^c in Ref. 15 are also included in this graph for comparison.

Based on the above results, we want to continue the discussion on the flux-pinning mechanism in MgB_2 . It seems that there are three regions in the field dependence of J_{cm} for single-crystal sample, constant J_{cm} at lower fields, power field dependence at the intermediate fields, and exponential

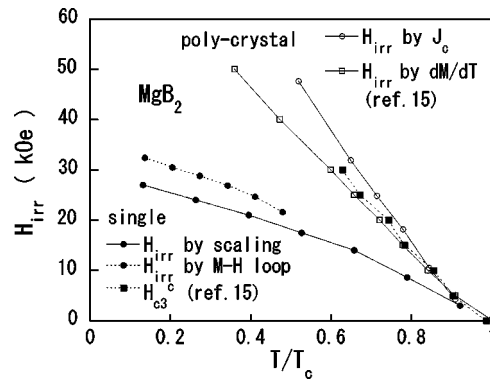


FIG. 9. Temperature-dependent irreversibility fields for polycrystalline (opened symbols) and single-crystalline (closed symbols) samples derived from J_{cm} in Fig. 4(a), zero points of dM/dT curves in Ref. 15, scaling behavior in Fig. 6(b) and the closed points in MHLs in Fig. 8. The data of H_{c3}^c are from Ref. 15.

field dependence at higher fields. The sudden change from constant to power field dependence results in the small peak near zero field. One possible reason is that the self-field effect shifts the peak from zero field and results in constant J_{cm} in lower fields. The second possible reason is that the constant J_{cm} correspond to single-vortex pinning and the power field dependence J_{cm} correspond to small bundle vortex pinning and the change from single vortex to small bundle vortex results in the near zero-field peak. The third possible reason is that the small peak may be originated from the surface pinning in single crystal because the overall shape of MHL is very similar to that of powder sample. And the surface pinning may be related to the surface superconductivity in MgB_2 .^{15,21} The different temperature dependences of the peak values of the near zero-field peak and the main peak mean that the two peaks are caused by different mechanisms. The main peak can be fitted by Kramer model with $h_{peak} \approx 0.2$, which indicates that flux pinning in MgB_2 is not weak and the deformation of flux-line lattice changes from elastic one to plastic one at lower fields. Due to the high Ginzburg-Landau parameter $\kappa = 26$ in MgB_2 , the magnetic interaction is negligible and the core interaction, such as δl pinning or δT_c pinning, is very important. The linear temperature dependence of $F_{p,peak}$ suggests that the pinning mechanism is δT_c pinning. The pinning centers in single-crystal sample may be the crystal structural defects and impurity such as MgO with sizes comparative to the coherence length.

For polycrystalline sample, the pinning peak is also at about $B/B_{scaling} \approx 0.2$ though the scaling is not good. However, the pinning force density is about two orders higher than that in single-crystalline sample. This phenomenon may be explained by the following two origins.

(1) Flux-pinning mechanism is the same for the two kinds of samples while polycrystalline sample has more pinning centers than single-crystalline sample, such as the grain boundaries due to the anisotropy of H_{c2} as reported in V_3Si .²⁵

(2) There may be normal-surface pinning in polycrystalline sample related to the surface superconductivity H_{c3} and anisotropy of H_{c2} . The H_{c3}^c for single-crystalline sample is almost the same as the irreversibility field of the polycrystalline sample as shown in Fig. 9, which may be the evidence for that the normal-surface pinning related to H_{c3}^c is the effective flux pinning in polycrystalline samples. The Kramer scaling is almost the same as the relation for normal-surface pinning, $f(b) \propto b^{1/2}(1-b)^2$, deduced from a simple summation of individual pinning forces theoretically.²⁶ So the pinning peak appears also at $B/B_{scaling} \approx 0.2$.

C. Anisotropy of flux pinning

For studying the anisotropy of flux pinning in MgB_2 , we have measured the angular dependent superconducting transition by standard four-probe method with field applied at different angles from c axis as shown in Fig. 10(a). The upper critical field H_{c2} and the irreversibility field H_{irr} as shown in Fig. 10(b) are determined by the peak point of $\partial R/\partial H$ curves and by the end point of transition (zero point of $\partial R/\partial H$) curves. The anisotropic behavior of irreversibility

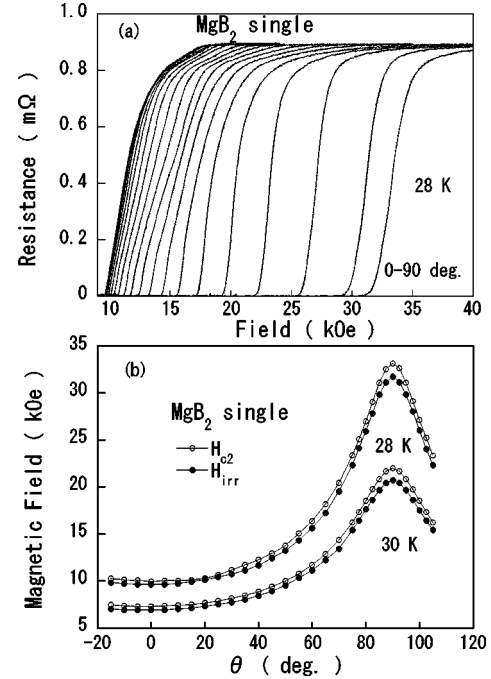


FIG. 10. (a) Typical transition curves by standard four-probe transport measurements with fields applied at different angles from c axis every 5° . (b) Angular dependence of irreversibility fields and upper critical fields determined from the transition curves.

field is almost the same as that of upper critical field, which indicates that the anisotropy of flux pinning is mainly determined by the anisotropy of superconductivity. It is also concluded that no directional pinning centers are effective at high fields near H_{irr} .

Recently, Takahashi *et al.* have reported an evidence for intrinsic pinning in Ref. 13. In that paper, they compare the angle-dependent magnetic hysteresis in the same magnetic field rather than the same reduced field without considering the anisotropy of H_{c2} . So it should be the anisotropic pinning force rather than intrinsic pinning to be claimed. In fact, the ratio of coherence length ξ_c to the layer spacing is about 8 for MgB_2 , while it is less than unity even in the least anisotropic high- T_c superconductor $\text{YBa}_2\text{Cu}_3\text{O}_7$. So the intrinsic pinning as proposed by Tachiki and Takahashi²⁷ will not give an appreciable contribution to J_c in MgB_2 . Our direct measurements of the anisotropic H_{irr} strongly support the absence of intrinsic pinning in MgB_2 .

IV. CONCLUSION

Flux-pinning properties of single-crystalline and polycrystalline MgB_2 have been studied and compared. Heating effect shows up even at relatively slow field-sweep rate of 100 Oe/s. Hence, the magnetic field should be applied slowly to measure the quasi-critical-state MHLs. The field dependence of critical current and flux pinning is different for single-crystalline and polycrystalline samples. There is only one pinning force peak for polycrystalline sample, whereas there are three pinning force peaks for single-crystalline

sample. There seems surface pinning in single crystals and normal-surface pinning in polycrystalline sample. The main pinning mechanism is identified as the δT_c core pinning by isotropic pinning centers such as point defects, impurities, and grain boundaries.

ACKNOWLEDGMENTS

This work was partly supported by a Grant-in-Aid for Scientific Research from the Ministry of Education, Culture, Sports, Science, and Technology, Japan.

-
- *Mailing address. Department of Applied Physics, The University of Tokyo, 7-3-1 Hongo, Bunkyo-ku, Tokyo 113-8656, Japan. Email address: tamegai@ap.t.u-tokyo.ac.jp
- ¹J. Nagamatsu, N. Nakagawa, T. Muranaka, Y. Zenitani, and J. Akimitsu, *Nature (London)* **410**, 63 (2001).
 - ²D.C. Larbalestier, M.O. Rikel, L.D. Cooley, A.A. Polyanskii, J.Y. Jiang, S. Patnaik, X.Y. Cai, D.M. Feldmann, A. Gurevich, A.A. Squitieri, M.T. Naus, C.B. Eom, E.E. Hellstrom, R.J. Cava, K.A. Regan, N. Rogado, M.A. Hayward, T. He, J.S. Slusky, P. Khalifah, K. Inumaru, and M. Haas, *Nature (London)* **410**, 186 (2001).
 - ³Hyeong-Jin Kim, W.N. Kang, Eun-Mi Choi, Mun-Seog Kim, Kijoon H.P. Kim, and Sung-Ik Lee, *Phys. Rev. Lett.* **87**, 087002 (2001).
 - ⁴Mun-Seog Kim, C.U. Jung, Min-Seok Park, S.Y. Lee, Kijoon H.P. Kim, W.N. Kang, and Sung-Ik Lee, *Phys. Rev. B* **64**, 012511 (2001).
 - ⁵S.X. Dou, X.L. Wang, J. Horvat, D. Milliken, E.W. Collings, and M.D. Sumption, *Physica C* **361**, 79 (2001).
 - ⁶M.J. Qin, X.L. Wang, H.K. Liu, and S.X. Dou, *Phys. Rev. B* **65**, 132508 (2002).
 - ⁷M. Xu, H. Kitazawa, Y. Takano, J. Ye, K. Nishida, H. Abe, A. Matsushita, and G. Kido, *Appl. Phys. Lett.* **79**, 2779 (2001).
 - ⁸Sergey Lee, Hatsumi Mori, Takahiko Masui, Yuri Eltsev, Ayako Yamamoto, and Setsuko Tajima, *J. Phys. Soc. Jpn.* **70**, 2255 (2001).
 - ⁹K.H.P. Kim, J.-H. Choi, C.U. Jung, P. Chowdhury, H.-S. Lee, M.-S. Park, H.-J. Kim, J.Y. Kim, Z. Du, E.M. Choi, M.-S. Kim, W.N. Kang, S. -IK Lee, G.Y. Sung, and J.Y. Lee, *Phys. Rev. B* **65**, 100510(R) (2002).
 - ¹⁰A.K. Pradhan, Z.X. Shi, M. Tokunaga, T. Tamegai, Y. Takano, K. Togano, H. Kito, and H. Ihara, *Phys. Rev. B* **64**, 212509 (2001).
 - ¹¹C.U. Jung, J.Y. Kim, P. Chowdhury, Kijoon H.P. Kim, Sung-IK Lee, D.S. Koh, N. Tamura, W.A. Caldwell, and J.R. Patel, *Phys. Rev. B* **66**, 184519 (2002).
 - ¹²M. Zehetmayer, M. Eisterer, J. Jun, S.M. Kazakov, J. Karpinski, A. Wisniewski, and H.W. Weber, *Phys. Rev. B* **66**, 052505 (2002).
 - ¹³Ken'ichi Takahashi, Toshiyuki Atsumi, Nariaki Yamamoto, Mingxiang Xu, Hideaki Kitazawa, and Takekazu Ishida, *Phys. Rev. B* **66**, 012501 (2002).
 - ¹⁴Y. Takano, H. Takeya, H. Fujii, H. Kumakura, T. Hatano, K. Togano, H. Kito, and H. Ihara, *Appl. Phys. Lett.* **78**, 2914 (2001).
 - ¹⁵Z.X. Shi, M. Tokunaga, T. Tamegai, Y. Takano, K. Togano, H. Kito, and H. Ihara, *Phys. Rev. B* **68**, 104513 (2003).
 - ¹⁶A.V. Bobyl, D.V. Shantsev, T.H. Johansen, W.N. Kang, H.J. Kim, E.M. Choi, and S.I. Lee, *Appl. Phys. Lett.* **80**, 4588 (2002).
 - ¹⁷T.H. Johansen, M. Baziljevich, D.V. Shantsev, P.E. Goa, Y.M. Galperin, W.N. Kang, H.J. Kim, E.M. Choi, M.-S. Kim, and S.I. Lee, *Supercond. Sci. Technol.* **14**, 726 (2001).
 - ¹⁸Z.X. Shi, M. Tokunaga, A.K. Pradhan, T. Tamegai, Y. Takano, K. Togano, H. Kito, and H. Ihara, *Physica C* **370**, 6 (2002).
 - ¹⁹Edward J. Kramer, *J. Appl. Phys.* **44**, 1360 (1973).
 - ²⁰Z.X. Shi, A.K. Pradhan, M. Tokunaga, K. Yamazaki, T. Tamegai, Y. Takano, K. Togano, H. Kito, and H. Ihara, *Physica C* **378-381**, 550 (2002).
 - ²¹U. Welp, A. Rydh, G. Karapetrov, W.K. Kwok, G.W. Crabtree, Ch. Marcenat, L. Paulius, T. Klein, J. Marcus, K.H.P. Kim, C.U. Jung, H.-S. Lee, B. Kang, and S.-I. Lee, *Phys. Rev. B* **67**, 012505 (2003).
 - ²²M. Angst, R. Puzniak, A. Wisniewski, J. Jun, S.M. Kazakov, and J. Karpinski, *Phys. Rev. B* **67**, 012502 (2003).
 - ²³L. Lyard, P. Samuely, P. Szabo, T. Klein, C. Marcenat, L. Paulius, K.H.P. Kim, C.U. Jung, H.-S. Lee, B. Kang, S. Choi, S.-I. Lee, J. Marcus, S. Blanchard, A.G. Jansen, U. Welp, G. Karapetrov, and W.K. Kwok, *Phys. Rev. B* **66**, 180502 (2002).
 - ²⁴T. Giamarchi and P.L. Doussal, *Phys. Rev. Lett.* **72**, 1530 (1994).
 - ²⁵Edward J. Kramer and G.S. Knapp, *J. Appl. Phys.* **46**, 4595 (1975).
 - ²⁶T. Matsushita, *Physica C* **205**, 289 (1993).
 - ²⁷M. Tachiki and S. Takahashi, *Solid State Commun.* **70**, 291 (1989).